01 Aug 2007

DHP-Based Wide-Area Coordinating Control of a Power System with a Large Wind Farm and Multiple FACTS Devices

Wei Qiao

Ganesh K. Venayagamoorthy
Missouri University of Science and Technology

Ronald G. Harley

Recommended Citation

W. Qiao et al., "DHP-Based Wide-Area Coordinating Control of a Power System with a Large Wind Farm and Multiple FACTS Devices," *Proceedings of International Joint Conference on Neural Networks, 2007*, Institute of Electrical and Electronics Engineers (IEEE), Aug 2007.
The definitive version is available at https://doi.org/10.1109/IJCNN.2007.4371281

Proceedings of International Joint Conference on Neural Networks, Orlando, Florida, USA, August 12-17, 2007

DHP-Based Wide-Area Coordinating Control of a Power System with a Large Wind Farm and Multiple FACTS Devices

Wei Qiao, Ganesh K. Venayagamoorthy, and Ronald G. Harley

***Abstract*—Wide-area coordinating control is becoming an important issue and a challenging problem in the power industry. This paper proposes a novel optimal wide-area monitor and wide-area coordinating neurocontroller (WACNC), based on wide-area measurements, for a power system with power system stabilizers, a large wind farm, and multiple flexible ac transmission system (FACTS) devices. The wide-area monitor is a radial basis function neural network (RBFNN) that identifies the input-output dynamics of the nonlinear power system. Its parameters are optimized through a particle swarm optimization (PSO) based method. The WACNC is designed by using the dual heuristic programming (DHP) method and RBFNNs. It operates at a global level to coordinate the actions of local power system controllers. Each local controller communicates with the WACNC, receives remote control signals from the WACNC to enhance its dynamic performance, and therefore helps improve system-wide dynamic and transient performance.**

I. Introduction

POWER systems are large-scale, nonlinear, non-stationary, multivariable, complex systems distributed over large geographic areas. System-wide disturbances in power systems are a challenging problem for the utility industry. On the other hand, because of new constraints placed by economical and environmental factors, the trend in power system planning and operation is toward maximum utilization of existing electricity infrastructure, with tight operating margins, and increased penetration of renewable energy sources such as wind power. Under these conditions, power systems become more complex to operate and to control, and, thus, more vulnerable to a disturbance [1]. When a major disturbance occurs, protection and control actions are required to stop the power system degradation, restore the system to a normal state, and minimize the impact of the disturbance.

The standard power system controllers, such as the generator exciter and automatic voltage regulator (AVR) [2], speed governor [2], PSS [2], and power electronics based FACTS devices [3], are local non-coordinated linear controllers. Each of them controls some local quantity to achieve a local optimal performance, but has no information on the entire system performance. Further, the possible interactions between these local controllers might lead to adverse effects causing inappropriate control effort by different controllers. As a result, when severe disturbances or contingencies occur, these local controllers are not always able to guarantee stability [4].

During the past two decades, much effort has been made by power engineers and control researchers to improve power system stability. With the increased availability of advanced computer, communication and measurement technologies (e.g., synchronized phasor measurement units (PMU) based on a global positioning satellite (GPS) system) [1], the development of wide-area coordinating control (WACC) is becoming feasible. A WACC based on wide-area measurements coordinates the actions of local controllers to achieve system-wide dynamic optimization and stability. Each local controller communicates with the WACC, reports to and receives coordination/control signals from the WACC, to help attain system-wide performance goals.

Designing the WACC needs knowledge of the entire power system dynamics to be available to the designers. Due to the large-scale, nonlinear, stochastic, and complex nature of power systems, the traditional mathematical tools and control techniques are not sufficient to design such a WACC. This problem can be overcome by using neural networks (NNs) and adaptive-critic-design (ACD) [5], [6] based intelligent optimal nonlinear control techniques. However, previous works on NNs and ACDs based controllers focused on the local control of individual power system devices [7]-[9]; no work has been reported on WACC for different types of devices in a power system with renewable energy generation.

This paper proposes a novel optimal WACNC for a power system with PSSs, a large wind farm, and FACTS devices. First, an optimal wide-area monitor is designed by using a RBFNN [9] and PSO [10], to identify the input-output dynamics of the nonlinear plant. Based on this optimal wide-area monitor, the DHP method [5], [6] and RBFNNs are then used to design the WACNC. It uses wide-area measurements and operates at a global level to coordinate the actions of the local synchronous generator (with PSS), wind farm, and FACTS controllers. Each local controller communicates with the WACNC, and receives remote control signals from the WACNC as external input(s), to help improve system-wide dynamic and transient performance.

II. Power System Model

The 4-machine 12-bus power system in [11] was proposed as a platform for studying FACTS device applications and integration of wind generation, and was extended in [12] to

This work was supported in part by the National Science Foundation, USA, under grant ECS # 0524183.

Wei Qiao and Ronald G. Harley are with the Intelligent Power Infrastructure Consortium (IPIC) in the School of Electrical and Computer Engineering, Georgia Institute of Technology, Atlanta, GA 30332-0250 USA (e-mail: {weiqiao, rharley}@ece.gatech.edu).

Ganesh K. Venayagamoorthy is with the Real-Time Power and Intelligent Systems Laboratory in the Department of Electrical and Computer Engineering, University of Missouri-Rolla, Rolla, MO 65409-0249 USA (e-mail: gkumar@ieee.org).

1-4244-1380-X/07/$25.00 ©2007 IEEE

include a large wind farm, a static synchronous compensator (STATCOM) [3] and a static synchronous series compensator (SSSC) [3], as shown in Fig. 1. The system covers three geographical areas. Area 1 is predominantly a generation area with most of its generation coming from hydro power (G1 and G2). Area 2, located between the main generation area (Area 1) and the main load center (Area 3), has a large wind farm (G4), but it is insufficient to meet local demand. Area 3, situated about 500 km from Area 1, is a load center with some thermal generation (G3). Further, since the generation units in Areas 2 and 3 have limited energy available, the system demand must often be satisfied through transmission. The transmission system consists of 230 kV transmission lines except for one 345 kV link (line 7-8) between Areas 1 and 3.

The STATCOM is a shunt connected FACTS device. It is placed at bus 4 in the load area (Area 3), for steady state and transient voltage support. This relieves the under-voltage problems in Area 3 [11]. The SSSC is a series FACTS device. It is placed at the bus 7 end of line 7-8 to regulate its power flow. This arrangement can relieve the possible transmission congestion on line 1-6 caused by some contingencies in Area 3 [11], [12]. Both synchronous generators G2 and G3 are equipped with PSSs to improve damping of the local generator rotor oscillation modes. The synchronous generator (with PSS), wind farm, SSSC, and STATCOM controllers are each designed at the local level using standard linear control techniques and local signals, but are coordinated by the WACNC at a global level to achieve the system-wide performance goals.

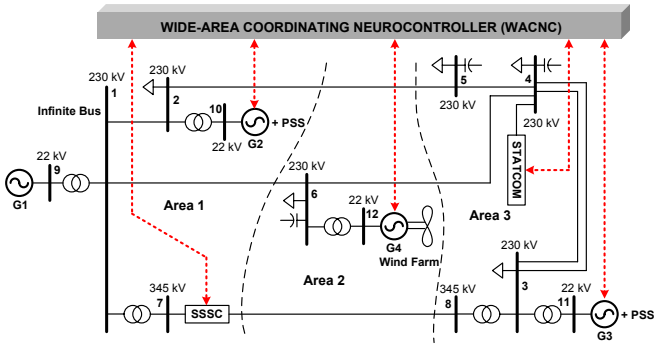

Fig. 1. Single-line diagram of the 4-machine 12-bus power system with a large wind farm, a STATCOM and an SSSC coordinated by a WACNC.

The system is simulated in the PSCAD/EMTDC environment. G1 is modeled as a three-phase infinite source, while the other two synchronous generators (G2 and G3) are modeled in detail, with the turbine governor and AVR/exciter (with PSS) dynamics taken into account. The function of each PSS is to improve the damping of its generator rotor oscillations by controlling its generator's excitation using auxiliary stabilizing signal(s), e.g., the deviation of generator rotor speed. A block diagram of a PSS is provided in [2]. The STATCOM and the SSSC are each modeled as a GTO PWM converter with a dc-link capacitor [12]. The detailed models and control schemes of the SSSC and STATCOM are given in [12].

The wind farm consists of over one hundred individual wind turbines. Each wind turbine is equipped with a doubly fed induction generator (DFIG) [12]. In this paper, the wind farm is represented by an aggregated model, namely, one equivalent DFIG driven by a single equivalent wind turbine [12], as shown in Fig. 2. Here the block "Grid" denotes the power network in Fig. 1 to which the wind farm is connected. The wound-rotor induction machine is fed from both stator and rotor sides. The stator is directly connected to the grid, while the rotor is connected to the grid through a variable frequency converter (VFC). The VFC consists of two IGBT PWM converters (the rotor-side converter RSC and the grid-side converter GSC) connected back-to-back by a dc-link capacitor. The crow-bar is used to protect the RSC from over-current in the rotor circuit during grid faults. Control of the DFIG is achieved by control of the RSC and GSC. The detailed control schemes of the RSC and the GSC are provided in [12].

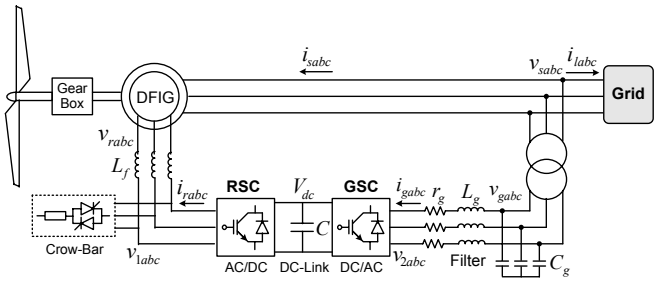

Fig. 2. Aggregated wind farm model: one equivalent DFIG driven by a single equivalent wind turbine.

III. Design of the WACNC

Figure 3 shows the schematic diagram of the proposed WACNC which coordinates different local controllers of the synchronous generators, wind farm, STATCOM, and SSSC. The WACNC operates at a global level, e.g., the control center of a power system. It receives remote signals from different devices over wide areas in the power system, such as signals from G2 (speed deviation $\Delta\omega_2$), G3 (speed deviation $\Delta\omega_3$), wind farm G4 (output active power deviation ΔP_{g4} and voltage deviation ΔV_6 at bus 6), SSSC (active power deviation ΔP_{78} of line 7-8 to which the SSSC is connected), and STATCOM (active power deviation ΔP_{54} of line 5-4 that is connected to the STATCOM bus 4). These remote signals contain the important dynamic/transient information of these devices and the power network. The use of ΔV_6 is because of its direct coupling with the wind farm reactive power. The remote signals, $\Delta\omega_2$, $\Delta\omega_3$, ΔV_6, ΔP_{g4}, ΔP_{78}, ΔP_{54}, are fed into the WACNC to generate a set of global optimal control signals, ΔV_{T2}, ΔV_{T3}, ΔQ_s, ΔQ_g, ΔV_4, ΔX_C. They are then used as the auxiliary input signals to coordinate the actions of local controllers. When a disturbance occurs, the coordination by the WACNC ensures that the power system returns back to the desired operating point as fast as possible after the disturbance with a minimum control effort. At local level, each local device is

controlled by its local controllers. These local controllers use both local signals and auxiliary remote control signals from the WACNC to achieve local as well as global dynamic and transient performance improvement of the power system.

For instance, for the reactive power control of the wind farm RSC, the command Q_s^* is the summation of two terms, Q_{s0} and ΔQ_s. The fixed set-point value Q_{s0} is determined by the local reactive power demand while taking into account the limit of the RSC rating. The supplementary command ΔQ_s is a remote signal generated by the WACNC, which enhances the dynamic performance of the local controller.

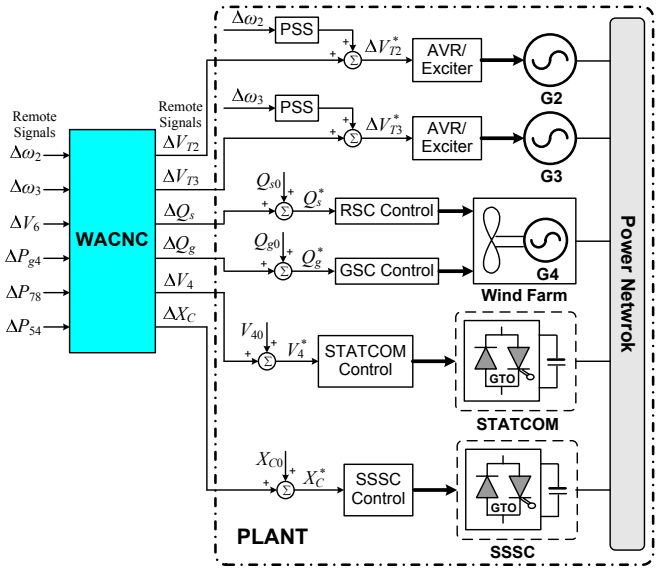

Fig. 3. Schematic diagram of the synchronous generator, wind farm, STATCOM, and SSSC local controllers coordinated by the WACNC.

The transfer functions between (ΔV_{T2}, ΔV_{T3}, ΔQ_s, ΔQ_g, ΔV_4, ΔX_C) and ($\Delta\omega_2$, $\Delta\omega_3$, ΔV_6, ΔP_{g4}, ΔP_{78}, ΔP_{54}) are complicated, nonlinear and depend on the network topology. To avoid having to derive such analytical functions, an ACD approach – DHP, and RBFNNs are used to design the WACNC. By employing the GPS synchronized PMUs, it is possible to deliver remote synchronized real-time signals to the control center at a speed of as high as 60 Hz sampling rate [1]. In this paper, the sampling rate for the WACNC implementation is chosen as 50 Hz in order to meet the PMU requirements for delivering the synchronized signals. Design of the WACNC should take into account the dynamics of local controllers. Therefore, the plant to be controlled includes the power network, the local devices and their controllers, as shown in the dash-dot-line block in Fig. 3.

A. Radial Basis Function Neural Network

The neural networks used in this paper are three-layer RBFNNs with a Gaussian density function as the activation function in the hidden layer. The overall input-output mapping of the RBFNN, $\hat{f}: X \in R^n \rightarrow Y \in R^m$ is

$$\hat{y}_i = b_i + \sum_{j=1}^{h} v_{ji} \exp\left(-\left\|x - C_j\right\|^2 / \beta_j^2\right) \qquad (1)$$

where x is the input vector; $C_j \in R^n$ and $\beta_j \in R$ are the center and width of the j^{th} RBF units in the hidden layer, respectively; h is the number of RBF units; b_i and v_{ji} are the bias term and the weight between hidden and output layers, respectively; and $\hat{y}_i$ is the i^{th} output.

B. Adaptive Critic Designs and DHP

Adaptive Critic Designs, proposed by Werbos [5], is a neural network based optimization and control technique which solves the classical nonlinear optimal control problems by combining concepts of *reinforcement learning* and *approximate dynamic programming*.

The DHP, belonging to the family of ACDs, requires three NNs for its implementation, one for the model (called wide-area monitor in this paper), one for the critic, and one for the action network [5]-[8]. The wide-area monitor is used to identify the input-output dynamics of the plant. The critic network estimates the derivatives of the cost-to-go function J with respect to the states of the plant Y, and J is given by

$$J(k) = \sum_{q=0}^{\infty} \gamma^q U(k+q) \qquad (2)$$

where $U(\cdot)$ is the utility function or one stage cost (user-defined function), and γ is a discount factor for finite horizon problems ($0<\gamma<1$). The ACD method determines optimal control laws for a system by successively adapting the critic and action networks. The adaptation process starts with a non-optimal control by the action network; the critic network then guides the action network towards the optimal solution at each successive adaptation. During the adaptations, neither of the networks needs any information of the desired control trajectory, only the desired cost needs to be known.

C. Design of the Optimal Wide-Area Monitor

The wide-area monitor is a three-layer RBFNN. The plant inputs $A = [\Delta V_{T2}, \Delta V_{T3}, \Delta Q_s, \Delta Q_g, \Delta V_4, \Delta X_C]$ and outputs $Y = [\Delta\omega_2, \Delta\omega_3, \Delta V_6, \Delta P_{g4}, \Delta P_{78}, \Delta P_{54}]$ at time instants k, k-1 and k-2 are fed into the wide-area monitor to estimate the plant outputs $\hat{Y} = [\Delta\hat{\omega}_2, \Delta\hat{\omega}_3, \Delta\hat{V}_6, \Delta\hat{P}_{g4}, \Delta\hat{P}_{78}, \Delta\hat{P}_{54}]$ at time k+1, as shown in Fig. 4. The wide-area monitor is an essential part for designing the WACNC because it provides a dynamic plant model for training the critic and action networks.

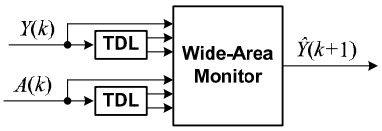

Fig. 4. Structure of the wide-area monitor: TDL denotes time delay lock.

The wide-area monitor is firstly pre-trained offline using a suitably selected training data set from two sets of training: *forced training* and *natural training* [7]-[9], over a wide system operating range.

The performance of RBFNNs relies on a set of parameters, including the number of RBF units, the RBF centers, widths, and the output weights. Given the number of RBF units, the locations of RBF centers are determined by a k-means

clustering algorithm [13] using the data from the training data set. After locating the RBF centers, a good method to determine the RBF widths is the *p*-nearest neighbors heuristic [14], in which the width β_i of the i^{th} RBF unit is given by:

$$\beta_i = \left(\frac{1}{p} \sum_{j=1}^{p} \left\| C_i - C_j \right\|^2 \right)^{1/2} \tag{3}$$

where C_j are the *p*-nearest neighbors to the center C_i. In this paper, *p* is chosen the same as the number of RBF units *h* in the hidden layer. After determining the RBF centers and widths, the output weights of the RBFNN are then calculated by singular value decomposition (SVD) method [16].

However, the widths given by (3) are still non-optimal. In [15], the authors have shown that the RBF widths can be optimized to achieve an optimal RBFNN with fewer RBF units and better performance. This section presents a method to design an optimal wide-area monitor by using PSO.

Suppose an initial width $\beta_i = \beta_{i,ini}$ of the i^{th} RBF unit has been calculated using (3), then the optimal width $\beta_{i,opt}$ can be defined by a set of equations, given by

$$\beta_{i,opt} = s_{i,opt} \cdot \beta_{i,ini} \quad i = 1, 2, \cdots, h \tag{4}$$

where $s_{i,opt} \in R$ is the optimal scaling factor for β_i. Now the problem becomes using PSO to find out the set of optimal scaling factors $s_{opt} = \{s_{i,opt}\}$ in the problem space. This is achieved by optimizing the following mean-square error (MSE) in dB over the training data set:

$$MSE = 10 \log \left(\sum_{k=1}^{N_T} \| Y(k) - \hat{Y}(k) \|^2 / N_T \right) \tag{5}$$

where N_T is the number of data samples in the training set, $Y(k)$ is the k^{th} output data sample in the training set; $\hat{Y}(k)$ is the k^{th} output sample from the wide-area monitor. The MSE in (5) is employed as the performance measure function for PSO implementation.

The MSEs over the selected training data set are plotted in Fig. 5 to show the performance of the wide-area monitor with the optimized widths but different numbers of RBF units. The minimum MSE is around -64 dB that can be achieved by using 35 or more RBF units, and any further increase over 35 does not improve the MSE significantly. Therefore, the optimal number of RBF units is chosen as 35 for the wide-area monitor.

Figure 6 shows the MSE as a function of the number of iterations in PSO during the RBF width optimization procedure for the wide-area monitor with 35 RBF units. The MSE at iteration no. 0, which denotes the RBFNN with initial widths form (3), is 280 dB. After 10 iterations, the MSE decreases to about -63 dB. These results indicate that the performance of the wide-area monitor is significantly improved by the proposed method. Further optimization using PSO with more than 10 iterations only slightly improves the MSE. Therefore, the optimal RBF widths can be found by PSO within only 10 iterations.

The final optimal wide-area monitor therefore has 35 RBF units, the RBF centers determined by *k*-means clustering algorithm, the optimized RBF widths found by PSO, and the output weights calculated by SVD method. It is now used for further implementation of the DHP.

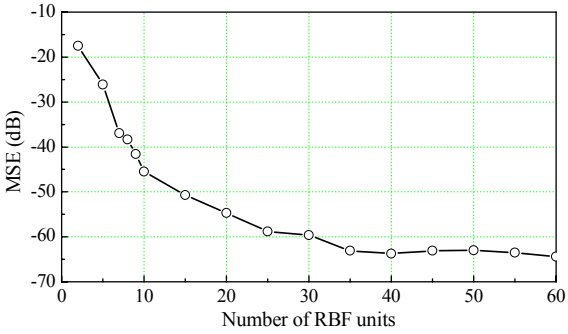

Fig. 5. Performance of the wide-area monitor with the optimized widths.

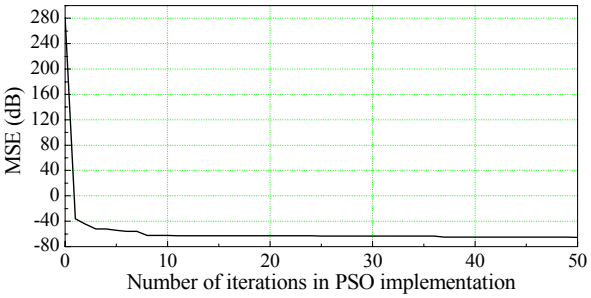

Fig. 6. Performance of the wide-area monitor with 35 RBF units during RBF width optimization procedure.

D. Design of the Critic Network

The critic network is a three-layer RBFNN. The inputs to the critic network are the estimated plant outputs, $\hat{Y}$ (from the wide-area monitor) and their two time-delayed values. The outputs of the critic network are the derivative, $\lambda = \partial J / \partial \hat{Y}$, of the function *J* in (2) with respect to the estimated plant outputs $\hat{Y}$, as shown in Fig. 7. The critic network learns to minimize the following error measure over time [6]:

$$\left\| E_C \right\| = \sum_k E_C^T(k) E_C(k) \tag{6}$$

where

$$E_C(k) = \frac{\partial J[\hat{Y}(k)]}{\partial \hat{Y}(k)} - \gamma \frac{\partial J[\hat{Y}(k+1)]}{\partial Y(k)} - \frac{\partial U(k)}{\partial Y(k)} \tag{7}$$

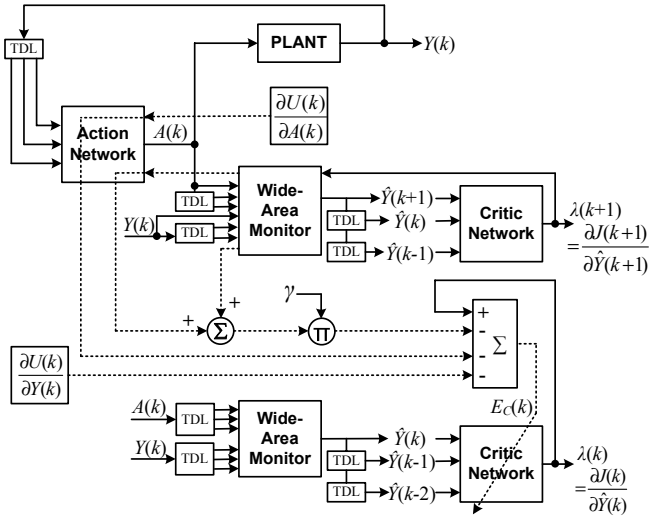

Fig. 7. Adaptation of the critic network in DHP

The utility function is defined as

$$U(k)=\frac{1}{2}\sum_{i=1}^{6}w_i[Y_i^2(k)+0.5Y_i^2(k-1)+0.1Y_i^2(k-2)] \quad (8)$$

where Y is the vector of the plant outputs, and w_i is a weighting factor for Y_i. Generally, two critic networks are required in DHP to estimate $\partial J/\partial \hat{Y}$ arising from the present state $\hat{Y}(k)$ and the future state $\hat{Y}(k+1)$. The adaptation of the critic network in DHP takes into account all relevant pathways of backpropagation as shown in Fig. 7. The output weights of the critic network are then updated by

$$\Delta W_C(k)=-\eta_C E_C^T(k)\frac{\partial^2 J[\hat{Y}(k)]}{\partial \hat{Y}(k)\partial W_C(k)} \quad (9)$$

where η_C is a positive learning gain.

E. Design of the Action Network

As shown in Fig. 8, the inputs to the action network are the plant outputs, Y, at time k-1, k-2 and k-3. The outputs of the action network are the plant inputs, A, at time k. The adaptation of the action network, is achieved by propagating $\lambda(k+1)$ back through the model to the action network [6]. The objective of such adaptation is to find out the optimal control trajectory A^* in order to minimize the cost-to-go function J over time, given by

$$A^*(k)=\arg\min_u[J(k)]=\arg\min_u[U(k)+\gamma J(k+1)] \quad (10)$$

The output weights of the action network are then updated by

$$\Delta W_A(k)=-\eta_A\left[\frac{\partial U(k)}{\partial A(k)}+\gamma\frac{\partial J(k+1)}{\partial A(k)}\right]^T\frac{\partial A(k)}{\partial W_A(k)} \quad (11)$$

The detailed training procedure of the critic and action networks can be found in [6]-[8].

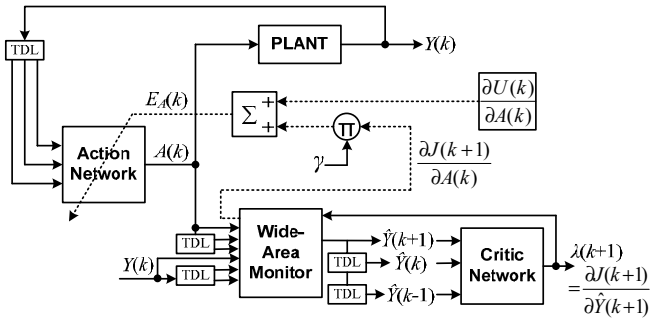

Fig. 8. Adaptation of the action network in DHP

IV. Simulation Results

Simulation studies are carried out to demonstrate the effectiveness of the WACNC during transient disturbances. The power system in Fig. 1 is operated at a normal operating condition (OP-I) as specified in [12], where the active power generated by the wind farm is P_{g4} = 300 MW. Thereafter at t = 51 s, a three-phase short circuit is applied to the bus 7 end of line 7-8, which is a critical transmission line connecting Area 1 and Area 3. The fault is cleared after 150 ms.

A. Online Monitoring Results

The proposed optimal wide-area monitor with the fixed parameters obtained from the offline training is applied to track the plant output dynamics online during this transient event. Figure 9 compares the estimated values of the plant outputs from the wide-area monitor, $\Delta\hat{\omega}_2$, $\Delta\hat{\omega}_3$, $\Delta\hat{P}_{g4}$, with the actual plant outputs, $\Delta\omega_2$, $\Delta\omega_3$, ΔP_{g4}. These results show that the wide-area monitor tracks the dynamics of the plant outputs online with good precision, without the need of any online adaptation at this operating point. This provides a good plant model for the adaptation of the critic and action networks in the DHP.

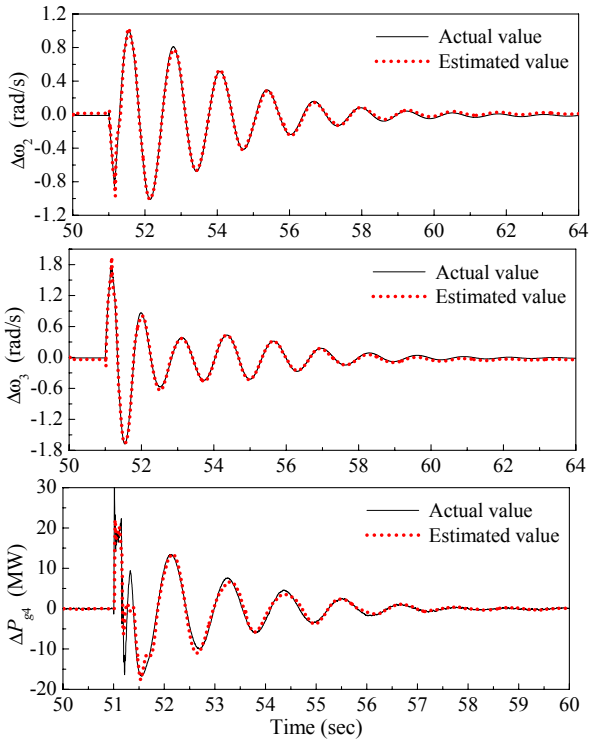

Fig. 9. Online monitoring results by the optimal wide-area monitor.

B. Power System Dynamic Performance Improvement Using the WACNC

The dynamic performance of the power system, reinforced with the WACNC, is compared with the case without the WACNC. Figure 10 shows the responses of $\Delta\omega_2$, $\Delta\omega_3$, and ΔP_{g4} with and without the WACNC. The WACNC improves rotor oscillation damping of synchronous generators (G1 and G2) and power oscillation damping of the wind farm (G4). It is well known that synchronous generators are key components for power system stability. In addition, with the increased penetration of wind generation, the transient behavior of wind farms during grid disturbances begins to influence the stability of the associated power system. Figure 10 shows important results that the WACNC has the capability to improve the transient performance of all generation units in a power system, and therefore the overall power system stability. These results are expected because the WACNC is designed at a global level to optimize the entire power system performance. This system-wide damping performance improvement, however, could not be achieved by any single local controller.

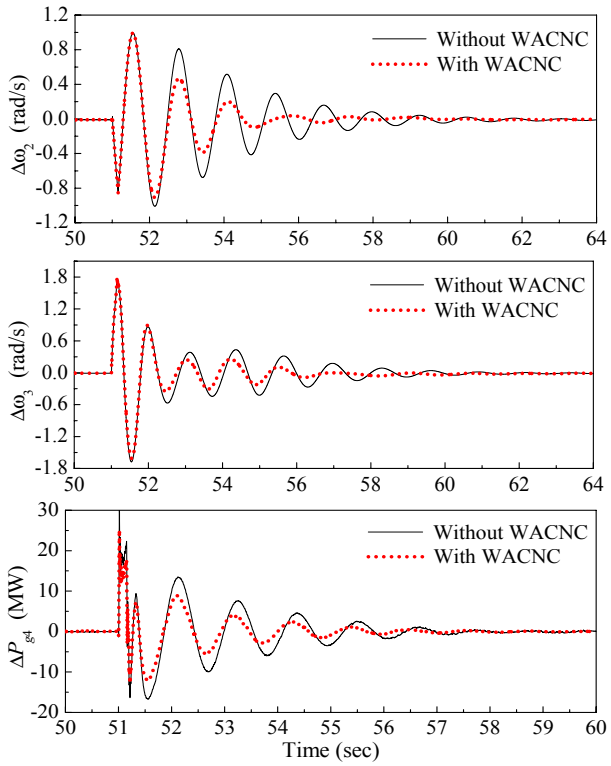

Fig. 10. Comparison of power system dynamic performance with and without the WACNC.

The same 150 ms three-phase short circuit test as for OP-I is applied at another operating condition (OP-II), where the active power generated by the wind farm becomes P_{g4} = 350 MW. Applying Prony analysis on the simulation waveforms, the eigenvalues, frequencies, and damping ratios of the dominant oscillation modes in ω_2 and ω_3 can be obtained, as shown in Table I. At both operating conditions, the WACNC improves the rotor oscillation damping of both synchronous generators. This indicates that the WACNC increases the stability margin of the entire power system, and therefore more active power can be transmitted to the loads while maintaining the system stable during transient disturbances.

TABLE I
DOMINANT MODES OF OSCILLATIONS IN ω_2 AND ω_3

		Signal	Eigenvalues $\lambda = \sigma \pm j\omega$	Frequency (Hz)	Damping ratio (%)
OP-I	Without WACNC	ω_2	-0.539 ± *j*5.174	0.83	10.36
		ω_3	-0.874 ± *j*7.320	1.17	11.85
	With WACNC	ω_2	-0.893 ± *j*5.344	0.86	16.48
		ω_3	-1.141 ± *j*7.740	1.24	14.59
OP-II	Without WACNC	ω_2	-0.732 ± *j*5.232	0.84	13.86
		ω_3	-0.683 ± *j*5.890	0.94	11.52
	With WACNC	ω_2	-1.054 ± *j*5.443	0.88	19.01
		ω_3	-0.806 ± *j*6.435	1.03	12.44

V. CONCLUSION

Wide-area coordinating control is becoming an important issue in power industry. This paper proposes a novel wide-area measurements based optimal wide-area monitor and WACNC, for a power system with PSSs, a large wind farm, and FACTS devices. The wide-area monitor, which identifies the input-output dynamics of the nonlinear power system, is a PSO-optimized RBFNN. Based on the optimal wide-area monitor, the DHP method and RBFNNs are employed to design the WACNC. It operates at a global level to coordinate the actions of local power system controllers. Each local controller receives remote control signals from the WACNC to help improve system-wide dynamic and transient performance.

Simulation studies are carried out to evaluate the dynamic performance of the WACNC during transient events. Results show that the WACNC improves damping of all the generating units in the power system and therefore the entire power system transient performance. To the authors' knowledge, this is the first paper on neural network based wide-area coordinating control for different types of devices in a power system which includes considering renewable energy generation.

REFERENCES

[1] M. Begovic, D. Novosel, D. Karlsson, C. Henville, and G. Michel, "Wide-area protection and emergency control," *Proceedings of the IEEE*, vol. 93, no. 5, pp. 876-891, May 2005.

[2] P. Kundur, *Power System Stability and Control*, EPRI, New York: McGraw-Hill, 1994.

[3] N. G. Hingorani and L. Gyugyi, *Understanding FACTS: Concepts and Technology of Flexible AC Transmission Systems*, New York: IEEE Press, 2000.

[4] F. Okou, L. A. Dessaint, and O. Akhrif, "Power system stability enhancement using a wide-area signals based hierarchical controller," *IEEE Trans. Power Systems*, vol. 20, no. 3, pp. 1465-1477, Aug. 2005.

[5] P. J. Werbos, "Approximate dynamic programming for real-time control and neural modeling," in *Handbook of Intelligent Control*, D. White and D. Sofge, Eds., New York: Van Nostrand Reinhold, 1992, pp. 493-526.

[6] D. V. Prokhorov and D. C. Wunsch, "Adaptive critic designs," *IEEE Trans. Neural Networks*, vol. 8, no. 5, pp. 997-1007, Sept. 1997.

[7] G. K. Venayagamoorthy, R. G. Harley, and D. C. Wunsch, "Implementation of adaptive critic-based neurocontrollers for turbogenerators in a multimachine power system," *IEEE Trans. Neural Networks*, vol. 14, no. 5, pp. 1047-1064, Sept. 2003.

[8] J-W Park, R. G. Harley, and G. K. Venayagamoorthy, "New External Neuro-controller for Series Capacitive Reactance Compensator in a Power Network," *IEEE Trans. Power Systems*, vol. 19, no. 3, pp. 1462-1472, Aug. 2004.

[9] W. Qiao and R. G. Harley, "Indirect adaptive external neuro-control for a series capacitive reactance compensator based on a voltage source PWM converter in damping power oscillations," *IEEE Trans. Industrial Electronics*, vol. 54, no. 1, Feb. 2007, in press.

[10] J. Kennedy and R. C. Eberhart, "Particle swarm optimization," in *Proc. of IEEE International Conference on Neural Networks*, Piscataway, NJ, USA, Nov. 27-Dec. 1, 1995, vol. 4, pp. 1942-1948.

[11] S. Jiang, U. D. Annakkage, and A. M. Gole, "A platform for validation of FACTS models," *IEEE Trans. Power Delivery*, vol. 21, no. 1, pp. 484-491, Jan. 2006.

[12] W. Qiao, R. G. Harley and G. K. Venayagamoorthy, "Effects of FACTS devices on a power system which includes a large wind farm," in *Proc. IEEE PES Power System Conference and Exposition*, Atlanta, GA, USA, Oct. 29-Nov. 1, 2006, pp. 2070-2076.

[13] K. Alsabti, S. Ranka, and V. Singh, "An efficient k-means clustering algorithm," in *Proc. First Workshop on High Performance Data Mining*, Orlando, FL, USA, Mar. 1998.

[14] J. Moody and C. J. Darken, "Fast learning in networks of locally-tuned processing units," *Neural Computation*, vol. 1, pp. 281-294, 1989.

[15] W. Qiao and R. G. Harley, "Optimization of radial basis function widths using particle swarm optimization," in *Proc. 2006 IEEE Swarm Intelligence Symposium*, Indianapolis, Indiana, USA, May 12-14, 2006.

[16] S. S. Haykin, *Neural Networks: A Comprehensive Foundation*, Prentice Hall, 2nd Edition, 1998.